doi:10.1246/cl.2011.255
Published on the web February 5, 2011

Conductive Atomic Force Microscopy of Chemically Synthesized Graphene Oxide and Interlayer Conduction

Yoshio Kanamori,[1] Seiji Obata,[1] and Koichiro Saiki*[1,2]
[1]*Department of Chemistry, School of Science, The University of Tokyo, 5-1-5 Kashiwanoha, Kashiwa, Chiba 277-8561*
[2]*Department of Complexity Science and Engineering, Graduate School of Frontier Sciences, The University of Tokyo, 5-1-5 Kashiwanoha, Kashiwa, Chiba 277-8561*

(Received November 17, 2010; CL-100971; E-mail: saiki@k.u-tokyo.ac.jp)

Graphene oxide, a chemically modified graphene, has been attracting wide attention because of promising adaptability to a wide variety of applications. However, the properties of graphene oxide itself are not known well. Using a conductive cantilever, we observed a current image of graphene oxide nanosheets of various thicknesses. Current–voltage characteristics were found to reflect the local conductivity normal to the nanosheets. Under high electric fields, the conduction was well described in terms of Poole–Frenkel emission mechanism. The fitting of *I–V* curves to the Poole–Frenkel model provides information on dielectric properties, and the relative permittivity of graphene oxide was found to be 4.8 ± 0.8.

Recently, graphene has attracted great attention due to its unique electronic, mechanical, and thermal properties. Several synthesis methods for graphene have been reported, including mechanical exfoliation of bulk graphite,[1] chemical vapor deposition (CVD),[2,3] and reduction of graphene oxide (GO).[4] Among these methods, oxidation of graphite powder giving GO sheets dispersed in solution is considered to be appropriate for large volume production. Apart from graphene, GO and its derivatives are expected to be applied to transparent electrodes in electroluminescence or photovoltaic devices,[5] memory FETs,[6] and catalysts.[7]

The preparation of GO and the properties of reduced GO have been studied intensively. Considerable work has been published over the past few years.[4] With regard to the structure or chemical composition of GO, there has been a consensus that several types of functional groups such as epoxide, hydroxy, carbonyl, and carboxyl exist in the GO plane and the effective thickness is greater than that of graphene. In contrast to the above work, only a limited number of reports are available concerning the electrical or optical properties of GO. The band gap of GO[8] and the refractive index of GO[9] have been reported previously.

In the present work, we observed the morphology of GO by use of atomic force microscopy with a conductive cantilever. Topographic and current images were obtained simultaneously. The similarity between both images indicates that current does not diffuse laterally beyond the spatial resolution of images (0.05 μm) but flows normally to the GO nanosheets. Thus, dependence of the conductivity on the electric field and the GO thickness provides information on electric transport perpendicular to the graphene sheets. Interlayer conduction of GO nanosheets could be explained in terms of the Poole–Frenkel model in high electric fields.

GO was prepared from natural graphite powder (SEC carbon) by the modified Hummers method.[10,11] Briefly, graphite powder, $NaNO_3$, and H_2SO_4 were placed in a flask, and the mixture was stirred while being cooled in an ice/water bath. $KMnO_4$ was then added gradually over about 1 h. Cooling was completed in 2 h, and the mixture was allowed to stand for 5 days at 20 °C with gentle stirring. The oxidized product was purified by rinsing with H_2SO_4 and H_2O_2 solutions repeatedly. In our experiment, GO flakes were dispersed in methanol after solvent substitution. The solution was centrifuged and the final product was supernatant fluid containing GO sheets with various thicknesses (monolayer to a few layers). A highly doped Si substrate was then dipped in the dispersion liquid and lifted. Mild centrifugation during the preparation or repeated dipping yielded thicker GO sheets on the Si substrate.[12] The final products were characterized by XPS. The atomic ratio of O/C was estimated to be 0.4–0.5, which is in good agreement with a previous report.[4]

Topographic and current images of GO sheets were measured with a scanning probe microscope (JEOL JSPM-5200). A schematic diagram of the measuring system is shown in Figure 1a. A Si substrate with GO was set on the mica plate attached to the piezo stage. By applying a bias voltage to the Si substrate, topographic and electric current images were obtained simultaneously. The current was measured by a preamplifier to the order of picoamperes. The images were obtained under high vacuum conditions ($<10^{-3}$ Pa) to prevent contamination of the probe. After measuring the topographic and current images, the cantilever was kept at a certain point on the GO sheet to

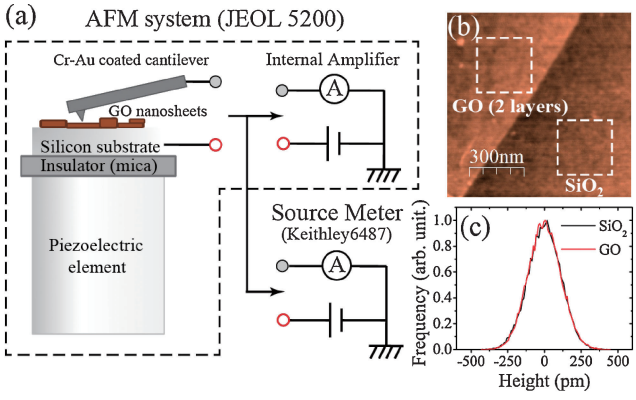

Figure 1. (a) A schematic diagram of the measurement system. The cantilever is connected to an internal amplifier for obtaining the current image and to a source meter for measuring *I–V* characteristics. (b) A noncontact AFM image (1 μm × 1 μm) of 2 layers GO. (c) Height distributions of GO and SiO_2 surfaces, which are measured in squares surrounded by white dashed lines in (b) (300 nm × 300 nm).

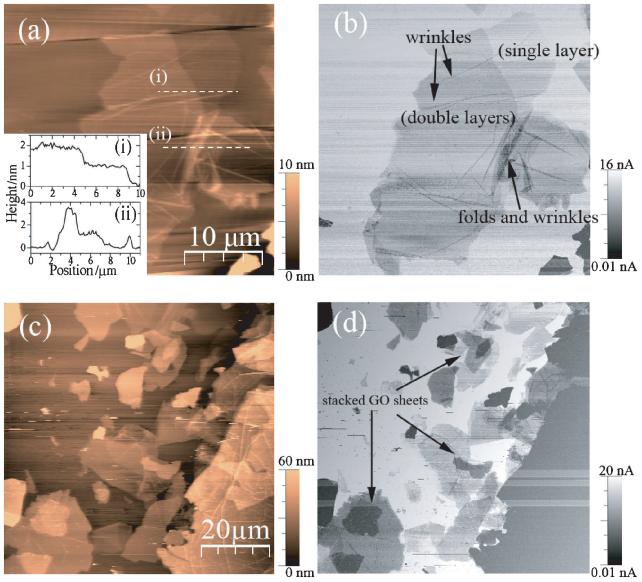

Figure 2. (a) A contact AFM image (35 μm × 35 μm) and (b) a current image of a few layers GO. Inset in (a) shows the height profiles taken along the white dashed lines. (c) A contact AFM image (80 μm × 80 μm) and (d) a current image of GO aggregates. The current image was taken with the sample-to-tip bias of +5 (b) and +10 V (d).

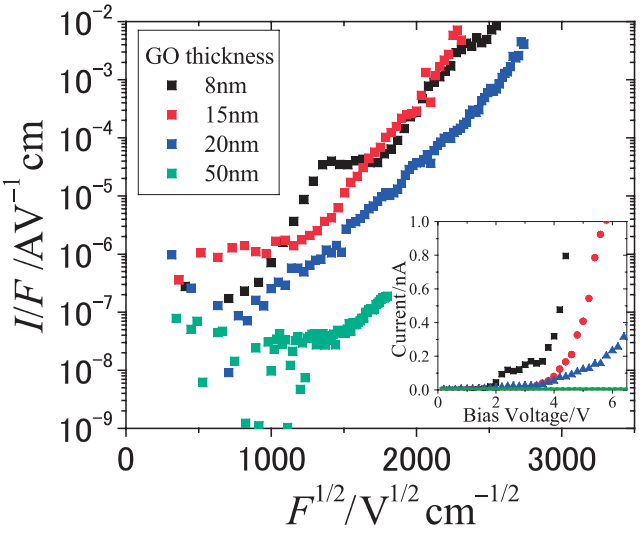

Figure 3. *I–V* characteristics of GO sheets with various thicknesses. The inset shows *I–V* curves in linear scale.

measure the current–voltage characteristics. The measurement was carried out by a source meter (Keithley model 6487) under ambient conditions. The contact force during *I–V* measurement was kept constant at 10 nN. The current gradually decreased during measurement, possibly because of the probe contamination by application of high voltages. Therefore, the cantilever was replaced by a new one before each measurement.

First, the flatness of the sheets was examined. In order to compare GO with SiO_2, GO was deposited on a SiO_2 (300 nm)/Si substrate. A typical AFM image of GO, which was measured in noncontact mode, is shown in Figure 1b. A height distribution which was measured both for GO and SiO_2 within the 300 nm squares (surrounded by white dashed lines in Figure 1b) is shown in Figure 1c. The curves are similar, indicating that the GO surface is as flat as that of SiO_2. The surface roughness of GO on SiO_2 is 0.2 nm, which is almost the same as the graphene on SiO_2.[13]

Contact AFM topographic images and current images of GO layers are depicted in Figure 2. A topographic image of a single and double GO layer is shown in Figure 2a together with the height profiles taken along the dashed lines (i) and (ii). The line (i) crosses a single GO step, the height of which is around 0.8 nm. The line (ii), on the other hand, crosses over the folds of GO sheet or the wrinkles on the GO surface, the height of which reaches a few nanometers.[14] The current image of the same area, which was measured at a bias voltage of 5 V, is shown in Figure 2b. Brighter areas correspond to higher electric current, in which the boundary between a single and double layer is clearly seen. It is noted that the spatial resolution in the current image is as high as that in the topographic image. Figure 2c shows a topographic image of GO aggregates. Thicker GO sheets ranging from 5 to 35 nm are observed. The corresponding current image measured at a bias voltage of 10 V is shown in Figure 2d. The contrast in the thicker region (bottom left) seems enhanced, while that in the thin region (bottom right) disappears. Thus, the contrast in the current image can be controlled by the applied voltage, taking account of the GO thickness. The results of Figures 2b and 2d show that the current images have resolution as high as the topographic images. This means that the current does not diffuse parallel to the GO sheet beyond the lateral resolution (less than 0.05 μm), which is consistant with the fact that the as grown GO is insulating for the electric field parallel to the sheet.[8]

After getting the topographic and current images, the cantilever was set at various positions on the flat GO sheets with different thicknesses, where local current–voltage (*I–V*) characteristics were measured. *I–V* characteristics of GO layers thinner than 8 nm showed fluctuations probably because the current is very sensitive to contact force.[15] The *I–V* characteristics of the GO layers thicker than 8 nm, however, were measured reproducibly and reversibly. Therefore, we focus on the GO layers thicker than 8 nm in the following discussion.

The inset of Figure 3 shows *I–V* characteristics, which indicate strong nonlinear behavior with applied voltage. The nonohmic conduction mechanism is often ascribed to the Schottky or Poole–Frenkel emission mechanism, which originates from lowering the potential barrier for carriers out of a defect center or a trap under an applied electric field. It has been reported that *I–V* curves in thin dielectrics can be fitted to a Schottky emission mechanism at low electric fields and a Poole–Frenkel conduction mechanism at high electric fields.[16] The current originating from Poole–Frenkel emission is described by eq 1,

$$I \propto F \exp\left(\frac{\sqrt{q^3 F/4\pi\varepsilon}}{kT}\right) \quad (1)$$

where F is an electric field applied normal to the GO sheet, ε is permittivity of GO, q is unit charge, and T is temperature. *I–V* characteristics are then plotted in semilog (I/F) vs. ($F^{1/2}$) for the GO layers with various thicknesses. At high electric fields, most

of points are on straight lines of the same slope, independently of the GO thickness from 8 to 50 nm. The good linear fit in semilog (I/F) vs. ($F^{1/2}$) plot indicates that the electric conduction normal to the GO layers at high electric fields is ascribed to Poole–Frenkel emission mechanism, although the deviation from the linear fit at low electric fields may originate from the contribution of Schottky emission mechanism. As the GO thickness increases, the I/F vs. $F^{1/2}$ curve deviates downward from the universal curve. The origin of the deviation is not definite at the present stage, while the decrease in effective electric field might be one of the reasons. Since the diameter of the probing cantilever is around 50 nm,[17] the electric field extends beyond the electrode for film thicker than a few tens of nanometers. For thinner film on the other hand, the electric field is confined just below the probing cantilever like a parallel plate capacitor.

The Poole–Frenkel type conduction has been reported in various insulators; SiO,[18] ZrO_2,[16] HfO_2,[19] and other materials. In these materials the donor-like electron trap sites are distributed continuously in the materials. In the case of GO, however, electrons are trapped in each GO layer, and they transit above the potential barrier between layers. In order to evaluate the trapping barrier height, temperature-dependent I–V measurement is required, which could not be achieved in the present work due to instrumental limitations.

Since the experimental I–V characteristics at high electric fields is well fitted by Poole–Frenkel model, the relative permittivity of GO can be estimated using eq 1. It is worth noting that the relative permittivity in eq 1 corresponds to that at the high frequency limit, or the square of refraction coefficient. Fitting (I/F)–($F^{1/2}$) plots by eq 1, the relative permittivity is calculated to be 4.8 ± 0.8 (assuming $T = 293$ K). This value is consistent with the calculated permittivity ($\varepsilon_r = 3.23$–4.76), based on the index of refraction and absorption of GO reported in ref 9.

The results mentioned above were obtained applying a positive bias voltage to the GO nanosheets. The dependence of current on the electric field and the GO thickness under negative bias is almost the same with that under positive bias, although the current intensity was slightly lower under the negative bias.

In summary, current images of GO nanosheets with various thicknesses were observed for the first time by a conductive cantilever of an AFM instrument. The current image is useful to monitor the GO thickness as well as wrinkles and folds in the nanosheet with high contrast. The current–voltage characteristics normal to the GO layers are well described in terms of the Poole–Frenkel emission mechanism, and the permittivity of GO can be evaluated from curve fitting.

This work was supported by a Grant-in-Aid for Scientific Research (No. 21360005) from the MEXT of Japan. One of the authors (Y.K.) acknowledge Global COE Program "Chemistry Innovation through Cooperation of Science and Engineering," MEXT, Japan, for their financial support.

References and Notes

1 K. S. Novoselov, A. K. Geim, S. V. Morozov, D. Jiang, Y. Zhang, S. V. Dubonos, I. V. Grigorieva, A. A. Firsov, *Science* **2004**, *306*, 666.
2 J. Hass, W. A. de Heer, E. H. Conrad, *J. Phys.: Condens. Matter* **2008**, *20*, 323202.
3 M. Yamamoto, S. Obata, K. Saiki, *Surf. Interface Anal.* **2010**, *42*, 1637.
4 D. R. Dreyer, S. Park, C. W. Bielawski, R. S. Ruoff, *Chem. Soc. Rev.* **2010**, *39*, 228.
5 G. Eda, Y.-Y. Lin, S. Miller, C.-W. Chen, W.-F. Su, M. Chhowalla, *Appl. Phys. Lett.* **2008**, *92*, 233305.
6 T.-W. Kim, Y. Gao, O. Acton, H.-L. Yip, H. Ma, H. Z. Chen, A. K.-Y. Jen, *Appl. Phys. Lett.* **2010**, *97*, 023310.
7 G. M. Scheuermann, L. Rumi, P. Steurer, W. Bannwarth, R. Mülhaupt, *J. Am. Chem. Soc.* **2009**, *131*, 8262.
8 X. Wu, M. Sprinkle, X. Li, F. Ming, C. Berger, W. A. de Heer, *Phys. Rev. Lett.* **2008**, *101*, 026801.
9 I. Jung, M. Vaupel, M. Pelton, R. Piner, D. A. Dikin, S. Stankovich, J. An, R. S. Ruoff, *J. Phys. Chem. C* **2008**, *112*, 8499.
10 W. S. Hummers, Jr., R. E. Offeman, *J. Am. Chem. Soc.* **1958**, *80*, 1339.
11 M. Hirata, T. Gotou, S. Horiuchi, M. Fujiwara, M. Ohba, *Carbon* **2004**, *42*, 2929.
12 S. Obata, H. Tanaka, H. Sato, K. Saiki, in preparation.
13 C. H. Lui, L. Liu, K. F. Mak, G. W. Flynn, T. F. Heinz, *Nature* **2009**, *462*, 339.
14 D. Pandey, R. Reifenberger, R. Piner, *Surf. Sci.* **2008**, *602*, 1607.
15 M. Lanza, M. Porti, M. Nafria, X. Aymerich, E. Whittaker, B. Hamilton, *Rev. Sci. Instrum.* **2010**, *81*, 106110.
16 J. P. Chang, Y.-S. Lin, *Appl. Phys. Lett.* **2001**, *79*, 3666.
17 From the cantilever data sheet.
18 T. E. Hartman, J. C. Blair, R. Bauer, *J. Appl. Phys.* **1966**, *37*, 2468.
19 D. S. Jeong, H. B. Park, C. S. Hwang, *Appl. Phys. Lett.* **2005**, *86*, 072903.

